Internal rotation and chlorine nuclear quadrupole coupling in 2-chloro-4-fluorotoluene explored by microwave spectroscopy and quantum chemistry

K P Rajappan Nair, Sven Herbers, William C Bailey, Daniel A Obenchain, Alberto Lesarri, Jens-Uwe Grabow, Ha Vinh Lam Nguyen

Internal rotation and chlorine nuclear quadrupole coupling in 2-chloro-4-fluorotoluene explored by microwave spectroscopy and quantum chemistry

K. P. Rajappan Nair,[a,b*] Sven Herbers,[a] William C. Bailey,[c] Daniel A. Obenchain,[a**] Alberto Lesarri,[d] Jens-Uwe Grabow,[a] and Ha Vinh Lam Nguyen[e,f*]

[a] Institut für Physikalische Chemie und Elektrochemie, Gottfried-Wilhelm-Leibniz-Universität Hannover, Callinstraße 3A, 30167 Hannover (Germany).

[b] Department of Atomic and Molecular Physics, Manipal Academy of Higher Education, Manipal, 576104, India.

[c] Chemistry-Physics Department, Kean University, 1000 Morris Avenue,Union, NJ, USA.

[d] Departamento de Química Física y Química Inorgánica – I.U. CINQUIMA, Facultad de Ciencias, Universidad de Valladolid, 47011 Valladolid (Spain).

[e] Laboratoire Interuniversitaire des Systèmes Atmosphériques (LISA), CNRS UMR 7583, Université Paris-Est Créteil, Université de Paris, Institut Pierre Simon Laplace, 61 avenue du Général de Gaulle, 94010 Créteil, France.

[f] Institut Universitaire de France (IUF), 1 rue Descartes, 75231 Paris cedex 05, France.

---

* Corresponding authors:

K. P. Rajappan Nair, e-mails: kprnair@gmail.com, kpr.nair@pci.uni-hannover.de

Ha Vinh Lam Nguyen, lam.nguyen@lisa.ipsl.fr

** Present address: Institut für Physikalische Chemie, Georg-August-Universität Göttingen, Tammanstraße 6, 37077 Göttingen, Germany.

Abstract

2-Chloro-4-fluorotoluene was investigated using a combination of molecular jet Fourier transform microwave spectroscopy in the frequency range from 5 to 21 GHz and quantum chemistry. The molecule experiences an internal rotation of the methyl group, which causes a fine splitting of all rotational transitions into doublets with separation on the order of a few tens of kHz. In addition, hyperfine effects originating from the chlorine nuclear quadrupole moment coupling its spin to the end-over-end rotation of the molecule are observed. The torsional barrier was derived using both the rho and the combined-axis-method, giving a value of 462.5(41) cm^{-1}. Accurate rotational constants and quadrupole coupling constants were determined for two ^{35}Cl and ^{37}Cl isotopologues and compared with Bailey's semi-experimental quantum chemical predictions. The gas phase molecular structure was deduced from the experimental rotational constants supplemented with those calculated by quantum chemistry at various levels of theory. The values of the methyl torsional barrier and chlorine nuclear quadrupole coupling constants were compared with the theoretical predictions and with those of other chlorotoluene derivatives.

Keywords: 2-chloro-4-fluortoluene, jet spectroscopy, microwave spectrum, internal rotation, chlorine nuclear quadrupole coupling

Graphical Abstract

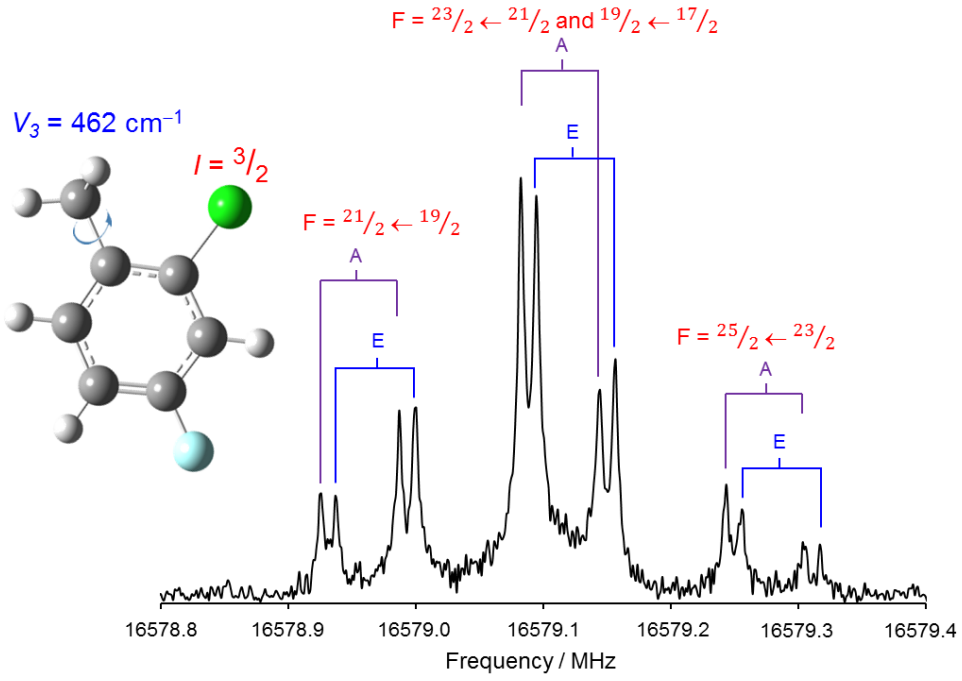

1. Introduction

Toluene and its derivatives provide a great challenge for spectroscopy in both experimental and theoretical work due to the low-barrier internal rotation arising from the methyl group. This effect causes a splitting of all rotational lines into torsional components in the microwave spectrum. A Hamiltonian model for a semi-rigid rotor is no longer sufficient, and additional terms accounting for the internal rotation need to be added. The determination of the internal rotation barriers offers insight into the changes in the electronic structure of toluene caused by the substituent effects. A vast number of fluoro substituted toluenes have been investigated, such as the three isomers of fluorotoluene [1-4], the six isomers of difluorotoluene [5-9], and 2,6-dimethylfluorobenzene [10], but studies on chloro-substituted toluenes are rather scarce. The reason is probably the quadrupole moment of the chlorine nucleus coupling the nuclear spin $I = 3/2$ to the end-over-end rotation of the molecule, thereby causing a hyperfine structure (hfs) in addition to the methyl torsional splittings. The simplest chlorine substituted toluene derivatives are the three chlorotoluenes. The microwave spectrum of *p*-chlorotoluene has been studied early in 1967 by Herberich [11] and then by Schubert et al. [12]. Investigations on the *o*-isomer were first performed using a Stark modulated spectrometer by Nair and Epple [13,14], but the small splittings arising from the methyl internal rotation could not be resolved. A few years later, the splittings were resolved using a molecular jet Fourier transform microwave (FTMW) spectrometer with higher resolution, and a torsional barrier of about 466 cm^{-1} could be deduced [15]. The study was subsequently extended to the millimeter wave region [16]. Recently, a reanalysis included both the microwave and millimeter wave data, and a barrier to internal rotation of about 469 cm^{-1} has been reported [17]. Finally, *m*-chlorotoluene has been recently investigated, revealing a nearly-free methyl torsion [18]. To our knowledge, no microwave spectroscopic studies on mixed halogen substituted toluenes like 2-chloro-4-fluorotoluene are available.

The implementation of the Hamiltonian including one methyl internal rotor and one weakly coupling nucleus can be treated with different approximations. The program *XIAM* [19], one of the codes most frequently used to deal with methyl internal rotation, uses a combined axis method where the Hamiltonian for the internal rotation of the methyl rotor is set up in the rho axis system and subsequently transformed into the principal axis system. A first order perturbation treatment is then applied to treat the nuclear quadrupole hyperfine structure, which is restricted to the

diagonal elements of the coupling tensor. While *XIAM* often does not experience difficulty with the ^{14}N nucleus [20-22], treatment of the chlorine hfs may be at the limit of the first-order perturbation method as the chlorine quadrupole coupling is stronger than that of ^{14}N. This is shown in the larger nuclear quadrupole coupling constants (NQCCs) of the chlorine nucleus compared to nitrogen in, e.g., cyanogen chloride with $\chi_{aa}^{^{35}Cl}$ = –83.27519(40) MHz and $\chi_{aa}^{^{14}N}$ = –3.62277(90) MHz [23], respectively. However, the number of studies on molecules with one methyl internal rotor and one chlorine nucleus is very limited to draw a conclusive statement on the performance of *XIAM* for this combination.

In the present work, we report the results obtained from the analysis of the molecular jet FTMW spectrum of 2-chloro-4-fluorotoluene. This work aims at determining the potential barrier hindering the methyl torsion when a chlorine atom is in close proximity of the methyl top as well as the NQCCs of the chlorine nucleus. We expect that the torsional barrier is largely influenced by electronic or steric effects and therefore would be similar to that of *o*-chlorotoluene [13-17]. However, it is possible that the presence of a fluorine atom in the conjugated π-bond system of the aromatic ring alters the barrier height and also the chlorine NQCCs. The performance of *XIAM* on methyl internal rotation treatment was checked against *RAM36hf* [24], an internal rotation program working exclusively in the rho axis system which also uses first order perturbation theory to treat the NQ-hfs. The fitting of the chlorine hfs was checked with the program *SPFIT/SPCAT* [25], which treats the hfs exactly by direct diagonalization of the Hamiltonian matrix rather than by perturbation theory, by exclusively fitting the A torsional symmetry species that follow an effective rigid-rotor pattern. The results of 2-chloro-4-fluorotoluene will serve as an important benchmark in the matrix of studies towards understanding of systematic trends in potential barriers and NQCCs of halogenated toluenes.

2. Quantum chemical calculations

2.1. Geometry optimizations

We performed optimizations using the B3LYP [26-28] and MP2 [29] methods in combination with Pople's triple-zeta basis set 6-311++G(2d,2p) [30] to predict the molecular geometry and rotational constants of 2-chloro-4-fluorotoluene. Only one conformer was obtained with the

optimized geometry given in Figure 1. The nuclear coordinates in the inertial principal axis system are available in Table S1 in the Supplementary Material. Subsequently, we repeated the optimizations at different levels of theory, additionally using the coupled cluster (CCSD) [31], Truhlar's M06-2X [32], and PBE0 (Perdew-Burke-Ernzerhof) [33] methods to evaluate the consistence of the calculations and to find the most effective method-basis set combination which yields the predicted rotational constants in best agreement with the experimental values. The results are summarized in Table S2 of the Supplementary Material. All calculations were carried out with the *Gaussian 16* program package [34].

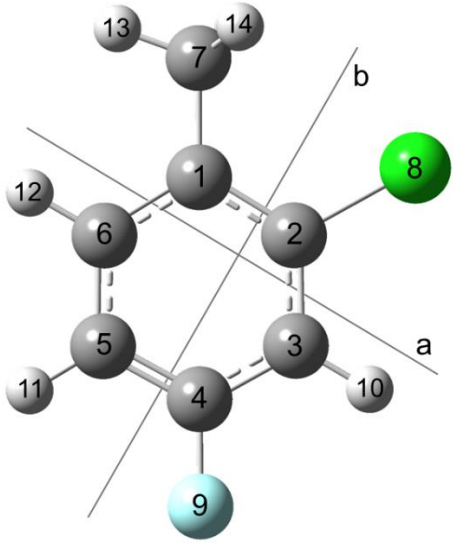

Figure 1: Projection onto the *ab*-plane of 2-chloro-4-fluorotoluene in its principal axis system. The molecular geometry was optimized at the MP2/6-311++G(2d,2p) level of theory (carbon = grey, hydrogen = white; chlorine = green, fluorine = light blue).

2.2. Methyl torsional barrier

The methyl torsional potential was predicted at the B3LYP and MP2/6-311++G(2d,2p) levels of theory by varying the internal rotation dihedral angle $\alpha = \angle(C_2,C_1,C_7,H_{13})$ in a grid of 10° while optimizing all other molecular parameters. We obtained a three-fold potential as illustrated in Figure 2, and the effective V_3 term, i.e. neglecting higher V_{3n} contributions, was predicted as 481.1 cm^{-1} and 391.5 cm^{-1}, respectively.

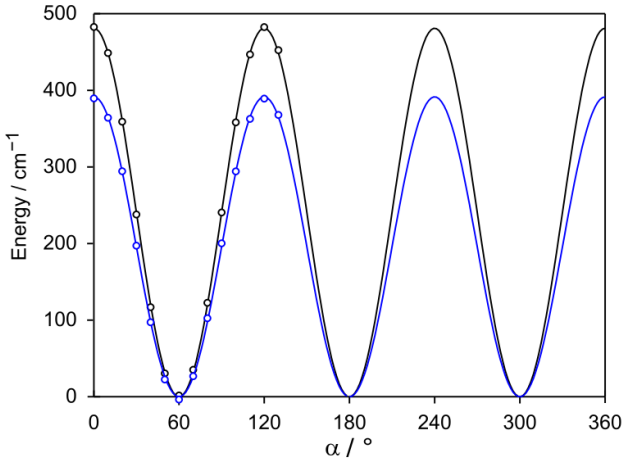

Figure 2: The potential energy curves of 2-chloro-4-fluorotoluene obtained by varying the internal rotation dihedral angle $\alpha = \angle(C_2,C_1,C_7,H_{13})$ in 10° steps calculated at the B3LYP/6-311++G(2d,2p) (blue curve) and MP2/6-311++G(2d,2p) levels of theory (black curve) levels of theory. Only the V_3 term was adjusted to fit the calculated energies. The predicted potential barriers are 391.5 cm^{-1} and 481.1 cm^{-1}, respectively

2.3. Chlorine nuclear quadrupole coupling constants

The components χ_{ij} of the nuclear quadrupole coupling tensor are proportional to those of the electric field gradient tensor (efg), q_{ij} by the relation

$$\chi_{ij} = (eQ/h) \cdot q_{ij}, \quad (1)$$

where e is the fundamental electric charge, Q is the nuclear electric quadrupole moment, and h is Planck's constant. In a number of previous studies, it has been found that the semi-experimental method introduced by Bailey [35,36] yielded rather reliable results for calculations of the NQCCs of many nuclei such as ^{14}N [37-39], ^{33}S [40], and ^{79}Br and ^{81}Br [41]. Therefore, we also apply it to calculate the NQCCs of the chlorine nucleus in 2-chloro-4-fluorotoluene. This cost-efficient method makes use of a calibration on a well-chosen level of molecular orbital calculation and experimental data. In the case of chlorine, we chose the Kohn-Sham density functional theory [26] employing Becke's one-parameter hybrid exchange functional and the Lee-Yang-Parr correlation functional (B1LYP) as implemented by Adamo and Barone [42,43]. Ahlrichs' bases TZV [44] are used in combination with the (3df,2p) polarization functions. These polarization functions are

those recommended for use with Pople's 6-311G bases [30], and were obtained online from the EMSL1 Basis Set Library [45,46].

There are two methods to determine the coefficient eQ/h of equation (1). With the first method, called the Q_{eff} method, the calculated efg q_{ij} on the experimental structures of a number of chlorine nucleus containing molecules were plotted against the corresponding experimental χ_{ij}, showing an almost perfectly linear regression for both the ^{35}Cl and the ^{37}Cl nuclei, as displayed in Figure 3. The coefficient eQ_{eff}/h is taken from the slope of the line as a best-fit parameter [34,35] with the value of −19.166(21) MHz/a.u. for the ^{35}Cl and −15.106(20) MHz/a.u. for the ^{37}Cl nucleus. The respective Q_{eff} values derived from the slopes are −81.568(91) mb and −64.292(86) mb, respectively.

The second method has eQ/h calculated directly from the values of Q = −81.65(80) mb and −64.35(64) mb for the ^{35}Cl and ^{37}Cl nucleus, respectively, given by Pyykkö and Li [47], yielding the respective conversion factors of −19.185 MHz/a.u. and −15.120 MHz/a.u. [36,48]. Since the conversion factors obtained with the two methods are very similar, we applied the second method for 2-chloro-4-fluorotoluene due to its larger simplicity.

Applying the efg calculations to the molecular geometry optimized at the MP2/6-311++G(2d,2p) level of theory, the nuclear quadrupole coupling tensor was determined with elements given in Table 1. As the symmetry was not constrained during the optimization, the resulting geometry slightly deviates from C_s symmetry, as reflected in the non-zero values of the *c*-coordinates (see Table S-1 of the Supplementary Material). Therefore, the values of χ_{ac}, though small, are not zero. For comparison, efg calculations were repeated on the PBE0/6-31G(3d,3p) optimized geometry, imposing C_s symmetry. The values of the NQCCs are also collected in Table 1. We note in all data points using for the calibration, the experimental diagonal elements of the chlorine quadrupole tensor possess consistently the opposite sign of the calculated constants. Since the signs of the diagonal elements could be determined unambiguously from the experiments, we adjusted the signs of the calculated NQCC values of 2-chloro-4-fluorotoluene to the opposite. The standard deviation of the residuals in the calibration is 0.49 MHz for ^{35}Cl and 0.44 MHz for ^{37}Cl, which was taken as the uncertainty in the calculations on NQCCs.

Table 1: Quadrupole coupling tensor elements (in MHz) in the principal inertial axis system predicted at the B1LYP/TZV(3df,2p)//MP2/6-311++G(2d,2p) level without symmetry constraints and B1LYP/TZV(3df,2p)//PBE0/6-31G(3d,3p) level implying C_s symmetry.

	MP2		PBE0	
NQCC	^{35}Cl	^{37}Cl	^{35}Cl	^{37}Cl
χ_{aa}	−40.38	−31.82	−39.33	−32.45
χ_{bb}	8.42	6.63	8.00	7.76
χ_{cc}	31.96	25.19	31.32	24.69
χ_{ab}	50.57	39.86	−50.33	−38.95
χ_{ac}	−0.01	−0.01	0	0
χ_{bc}	0.00	0.00	0	0

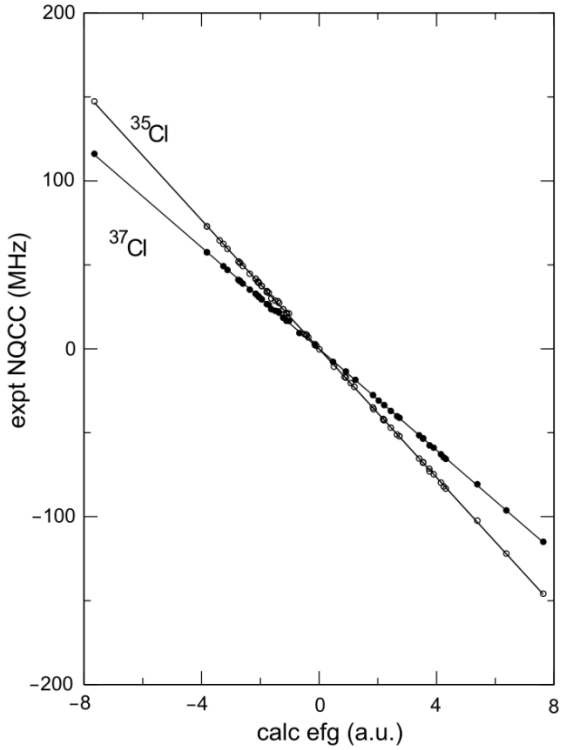

Figure 3: Linear regression of experimental NQCCs, χ_{ii}, versus B1LYP/TZV(3df,2p) predicted electric field gradients, q_{ii}. The slope, eQ/h, is −19.166(21) MHz/a.u. for the ^{35}Cl and −15.106(20) MHz/a.u. for the ^{37}Cl nucleus.

3. Rotational spectrum

3.1. Experimental

The spectra of 2-chloro-4-fluorotoluene were recorded using a molecular jet FTMW spectrometer with a coaxially oriented beam-resonator arrangement (COBRA) at Hannover University, Germany, which has been described previously [49]. The substance was purchased from Alfa-Aesar, and used as received (98% purity). The substance was kept in a small reservoir at the nozzle orifice to seed the carrier gas (neon or helium at stagnation pressures of 1-2 bar) before expansion into the resonator chamber. Velocity equilibration simultaneously reduces the collisional and the Doppler line broadening during the adiabatic expansion and also induces strong rovibrational cooling, leaving only the lowest-lying rovibrational levels populated. Therefore, the observed spectra are considerably simplified. All frequency measurements, referenced to a GPS-disciplined rubidium frequency standard, were performed between 5 and 21 GHz. The instrumental uncertainty for unblended lines is significantly less than its resolving power of 3 kHz. However, the effective measurement accuracy for 2-chloro-4-fluorotoluene may be larger since many lines appear slightly broader, attributable to unresolved proton spin-spin or spin-rotation coupling hfs. A typical spectrum is shown in Figure 4.

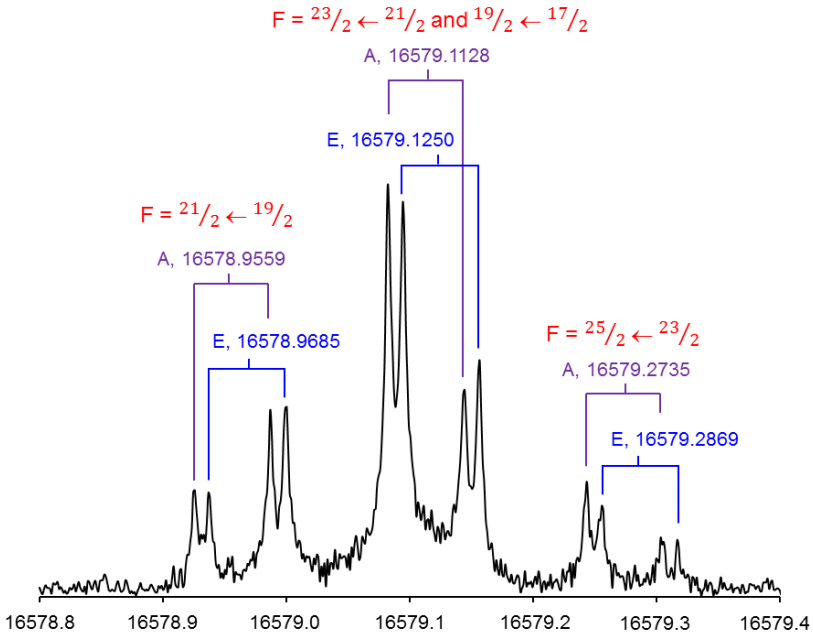

Figure 4: A typical high-resolution measurement of the $11_{0,11} - 10_{1,10}$ rotational transition of the ^{35}Cl isotopologue of 2-chloro-4-fluorotoluene (all frequencies in MHz). The Doppler doubling is marked by brackets with the mean values of the Doppler pairs being displayed. The torsional

symmetry species labels are placed before each frequency, and the chlorine quadrupole hyperfine component $F' \leftarrow F$ is given above each torsional A/E-splitting.

3.2. Spectral assignment and fits

A theoretical spectrum was predicted using the rotational constants and NQCCs obtained from calculations at the MP2/6-311++G(2d,2p) level of theory given in Section 2, taking into account the nuclear quadrupole interactions from the chlorine nucleus, while the effects of the methyl internal rotation were initially neglected. The electric dipole moment components predicted at the same level of theory were μ_a = 0.47 D, μ_b = 1.82 D, and μ_c = 0.00 D. Therefore, the spectrum was expected to be dominated by *b*-type transitions, accompanied by weak *a*-type transitions, and *c*-type transitions not to be observed. The estimated line positions were surveyed experimentally and lines could be found close to the expected positions. Each hyperfine component appears as a doublet (see Figure 4), which is the A-E doublet arising from the internal rotation of the C_3-symmetry methyl group. After a sufficient number of lines had been collected, we performed a fit with the *SPFIT/SPCAT* program [25] using the Hamiltonian for an asymmetric rotor (H_r) with centrifugal distortion corrections according to Watson's S-reduction (H_{cd}) [50] and a nuclear quadrupole term (H_Q) [51]:

$$H = H_r + H_{cd} + H_Q. \qquad (2)$$

H_Q depends on the quadrupole coupling tensor with the elements χ_{ij} of equation (1). The root-mean-square (rms) deviation of 4.0 kHz agrees well with the measurement accuracy and confirms the correct assignment of the A symmetry species as well as the hfs. The reasons for this conclusion is that (i) the A species can be fitted separately with sufficient accuracy using a semi-rigid asymmetric rotor Hamiltonian with quartic centrifugal distortion correction and (ii) the nuclear quadrupole coupling Hamiltonian direct-diagonalization treatment of *SPFIT/SPCAT* is exact even for the off-diagonal elements. However, non-diagonal NQC tensor elements were not determinable. Results from this A species fit are presented in Table 2.

Once the A symmetry species lines had been identified, we assigned the accompanying component of the narrow doublets on top of each hyperfine pattern to be the torsional E symmetry species. A global fit with the program *XIAM* [19] considered also the internal rotation angular momentum. The standard rigid frame-rigid top Hamiltonian (H_{ir}) and the empirical internal

rotation – overall rotation distortion term (H_{ird}) in the principal axis system were added to the terms given in equation (2):

$$H_{ir} = F\pi_\alpha^2 + \frac{V_3}{2}[1 - \cos(3\alpha)], \quad (3a)$$

$$H_{ird} = 2D_{\pi^2 J}\left(p_\alpha - \vec{\rho}^{+}\vec{P}\right)^2 P^2 + D_{\pi^2 K}\left\{\left(p_\alpha - \vec{\rho}^{+}\vec{P}\right)^2, P_a^2\right\}. \quad (3b)$$

In equation (3a), F is the reduced rotational constant of the methyl top, $\pi_\alpha = p_\alpha - \rho_a P_a - \rho_b P_b$ contains the angular momentum p_α of the methyl top conjugating to the internal rotation angle α and $\rho_g = \lambda_g I_\alpha / I_g$ with g = a, b and I_α the moment of inertia of the methyl top, I_g the components of principal moments of inertia of the molecule, and λ_g the direction cosines between the internal rotation axis i and the respective inertial axes. The latter term describes the hindering potential $V(\alpha)$. In equation (3b), $\vec{P}$ is the angular momentum vector along the rho axis and $\vec{\rho}^{+}$ the transposed rho vector. A fit including 40 rotational transitions with 78 A-E torsional symmetry species components and 231 quadrupole coupling components with F_0 fixed to the predicted value of 161.8404 GHz yielded an effective V_3 potential value of 462.5(41) cm^{-1} for the ^{35}Cl isotopologue. The fitted parameters are also presented in Table 2. The individual lines used in the fit are given in Table S-3 of the Supplementary Material. For the ^{37}Cl isotopologue, the values of the centrifugal distortion constants, the effective V_3 potential value, and the higher order parameters $D_{\pi^2 J}$ and $D_{\pi^2 K}$ are kept fixed to the results of the ^{35}Cl isotopologue fit, and only the three rotational constants, the NQCCs (χ_{aa} and $\chi_{bb}-\chi_{cc}$) together with the angle $\angle(i,a)$ between the internal rotor axis and the a-principal axis are optimized in the fit. The frequency list of the ^{37}Cl isotopologue is given in Table S-4. The rms deviations of the ^{35}Cl and ^{37}Cl fits are 4.8 kHz and 5.2 kHz, respectively, which are close to the measurement accuracy. We note that χ_{ab} can be determined in the A-species fit with *SPFIT/SPCAT*, but not in the global fit with *XIAM*. Fixing χ_{ab} to the predicted value of –50.33 MHz does not change neither the rms deviation nor the values of χ_{aa} and χ_{-} by more than their standard errors.

Finally, we evaluated the fit performance of the *XIAM* code with the program *RAM36hf* [24]. *RAM36* works exclusively in the rho axis system and can handle the torsion–rotation spectra of molecules with one methyl rotor and one quadrupole nucleus. Like *XIAM*, *RAM36hf* uses a first order perturbation treatment to treat the nuclear quadrupole hfs. However, an advantage of

RAM36hf is that effective high-order Hamiltonian terms dealing with the methyl internal rotation can be added from the input file, and interactions between different torsional states are considered.

Table 2: Molecular parameters of 2-chloro-4-fluorotoluene in the inertial principal axis system obtained from fits with the programs *SPFIT/SPCAT* and *XIAM*.

Par.[a]	Unit	^{35}Cl *SPFIT*[b]	^{35}Cl *XIAM*	$^{35}Cl_{calc.}$[c]	^{37}Cl *XIAM*
A	MHz	2281.82302(54)	2281.7986(28)	2284.0	2253.3845(33)
B	MHz	1047.76797(18)	1047.76472(61)	1042.6	1029.6237(15)
C	MHz	721.222677(33)	721.22131(12)	719.0	709.78299(16)
D_J	kHz	0.02280(71)	0.0190(18)	0.01948	0.0190[d]
D_{JK}	kHz	0.0383(25)		0.00295	
D_K	kHz	1.244(43)	1.02(15)	0.41958	1.0169[d]
d_1	kHz	–0.00733(37)	–0.0075(13)	–0.00724	–0.007458[d]
d_2	kHz	–0.0809(41)	–0.00179(40)	–0.00112	–0.001785[d]
F_0	GHz		161.8404[e]	161.8404	161.8404[e]
V_3	cm^{-1}		462.5(41)	481.1	462.4523[d]
$D_{\pi^2 J}$	MHz		0.1014(65)		0.101406[d]
$D_{\pi^2 K}$	MHz		–1.61(40)		–1.60877[d]
$\angle(i,a)$	°		44.7(16)	29.69	48.4(30)
$\angle(i,b)$	°		45.3(16)	60.30	41.6(30)
$\angle(i,c)$	°		90[f]	90.00	90[f]
χ_{aa}	MHz	–39.407(18)	–39.438(55)	–39.33	–32.34(16)
χ_{bb}	MHz	7.454(12)	7.472(43)	8.00	7.19(12)
χ_{cc}	MHz	31.953(21)	31.966(75)	31.32	25.15(19)
rms[g]	kHz	4.0	4.8		5.2
N_A/N_E[h]		129/0	129/102		64/59

[a] All parameters refer to the principal inertial axis system. Watson's S reduction and I^r representation were used. The D_{JK} quartic centrifugal distortion constant could not be determined in the *XIAM* fit. Standard errors are in units of the last digits.

[b] Including only the hyperfine components of the A symmetry species.

[c] Calculated at the MP2/6-311++G(2d,2p) level of theory except the NQCCs values which are predicted at the B1LYP/TZV(3df,2p)//PBE0/6-31G(3d,3p) level and corrected using the calibration factor –19.185 MHz/a.u. (see text). Centrifugal distortion constants are obtained from anharmonic frequency calculations at the B3LYP/6-311++G(2d,2p) level.

[d] Fixed to the value obtained from the ^{35}Cl isotopologue fit.

[e] Fixed to the calculated value.

[f] Fixed due to symmetry.

[g] Root-mean-square deviation of the fit.

[h] Number of torsional A and E symmetry species rotational components including the hyperfine nuclear quadrupole coupling components.

4. Results and discussion

Both ^{35}Cl and ^{37}Cl isotopic species were assigned for 2-chloro-4-fluorotoluene. When comparing the experimental rotational constants B_0 deduced from the *XIAM* fit, which refer to the vibrational ground state, with those obtained for the equilibrium structures B_e from geometry optimizations at different levels of theory, we typically find a good agreement with deviations of about 1 % or less (see Table S-2 of the Supplementary Material), especially when using Grimme's dispersion corrections [52] in combination with Pople's 6-311G(3df,3pd) basis set with or without diffuse function. Dunning's cc-pVTZ or aug-cc-pVTZ basis sets [53] in combination with the B3LYP method accidentally yield B_e constants which are in almost exact agreement with the experimental values. Although, strictly, a comparison of predicted B_e constants with experimental B_0 constants is not physically meaningful, it is practically useful for assignment purposes. In fact, the ground state rotational constants of A_0 = 2250.4 MHz, B_0 = 1039.3 MHz, and A_0 = 714.1 MHz predicted by anharmonic frequency calculations at the B3LYP/6-311++G(2d,2p) are not in better agreement, originating from error compensations in the optimizations which yield good accuracy accidentally. Apart from D_K also all centrifugal distortion constants are well-predicted.

The NQCCs of χ_{aa}, χ_{bb}, and χ_{cc} predicted at the B1LYP/TZV(3df,2p)//MP2/6-311++G(2d,2p) level are in satisfactory agreement with the experimental results for both ^{35}Cl and ^{37}Cl isotopologues. Calculations at the B1LYP/TZV(3df,2p)//PBE0/6-31G(3d,3p) level imposing C_s symmetry slightly improved the results. The χ_{cc} NQCC of the chlorine nucleus of 2-chloro-4-fluorotoluene can be compared directly with that of other molecules with C_s symmetry, because the principal c-axis is perpendicular to the molecular plane and collinear with one principal axis of the coupling tensor. The value χ_{cc} = –39.432 MHz found for the ^{35}Cl isotopologue of 2-chloro-4-fluorotoluene is much smaller than that found for 2-chlorotoluene (χ_{cc} = –67.972 MHz) [17] and 3-chlorotoluene (χ_{cc} = –60.325 MHz) [18]. This shows that not only the position of the methyl group but also the presence of a fluorine atom on the aromatic ring affects the nuclear quadrupole coupling of the chlorine nucleus, whereby the latter substituent has a much greater impact. The χ_{ab} NQCC could not be determined experimentally with sufficient accuracy in the case of 2-chloro-4-fluorotoluene. A similar observation was made for the ^{37}Cl isotopologue with respective χ_{cc} values of –25.157 MHz, –53.889 MHz [17], and –47.913 MHz [18] for the fluorine-substituted and the two unsubstituted chlorotoluenes.

Due to the very small splitting arising from the internal rotation of the methyl group, we noticed that the determination of the barrier height is prone to be sensitive to the set of parameters used in the fit and ranges from about 440 to 470 cm^{-1} using the program *XIAM*. Figure 5 summarizes the dependence of the effective V_3 value and rms deviation on the set of parameters used. The rms is slightly better if the H_{ird} term is included in the Hamiltonian, but the obtained V_3 value changes significantly, especially if the $D_{\pi^2 K}$ parameter is included. The correlation between V_3 and F_0 is essentially linear. Correlations also explain the unusually large deviation between the experimental angle $\angle(i,a)$ and its predicted value, changing significantly when using different sets of parameters.

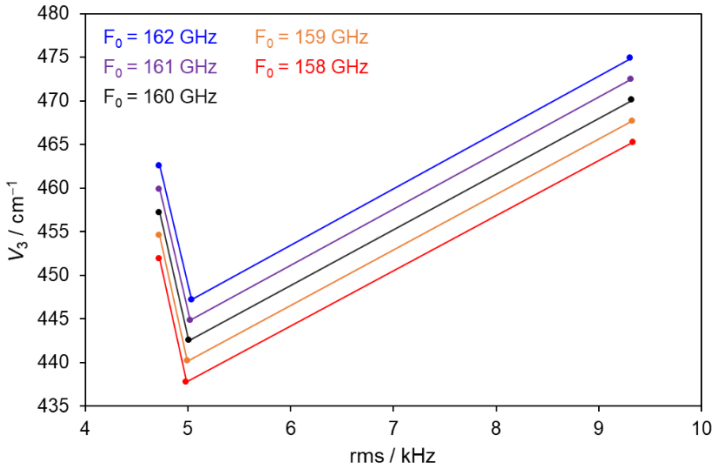

Figure 5: Root-mean-square deviation of the *XIAM* fit and the V_3 potential term obtained with different sets of parameters (see text).

In Figure 5 the rms deviations for different F_0 values are color-coded. The right hand side associates with the fits where only the physically meaningful geometry parameters, i.e. the rotational constants, the quartic centrifugal distortion constants, the NQCCs (χ_{aa} and $\chi_{bb}-\chi_{cc}$), the angle $\angle(i,a)$ between the internal rotor axis and the *a*-principal axis, and V_3, are fitted. The center of this representation corresponds to the fits where the $D_{\pi^2 J}$ parameter is included. The left hand side refers to fits where both $D_{\pi^2 J}$ and $D_{\pi^2 K}$ are fitted.

The rms deviation of the *XIAM* ^{35}Cl fit including both the A and E torsional species is 4.8 kHz, practically the same than that of 4.0 kHz obtained with *SPFIT/SPCAT* when only the A

species transitions are fitted. The program *RAM36* yields similar rms deviation similar to that obtained by *XIAM*. Since the torsional A symmetry species lines are known to follow a semi-rigid asymmetric rotor Hamiltonian with centrifugal distortion correction, we conclude that the slightly higher but satisfactory rms deviations of *XIAM* and *RAM36* arises from the perturbation treatment being at the limit for the hfs of the chlorine nucleus, while the exact treatment of nuclear quadrupole coupling of *SPFIT/SPCAT* results in an rms consistent with the line width of the observed transitions.

Comparing the V_3 potential barrier of 2-chloro-4-fluorotoluene (462 cm^{-1} with the data set reported in Table 2) to that of 2-chlorotoluene (469 cm^{-1}) [17], it is interesting to note that while the fluorine substitution at the *para*-position significantly affects the NQCCs of the chlorine nucleus, its effect on the potential barrier is small. Investigations of other halogenated toluenes will increase the empirical data required to provide a global view of the internal rotation and quadrupole coupling effects in this important class of compounds.

5. Conclusion

The rotational spectra of 2-chloro-4-fluorotoluene recorded using molecular jet Fourier transform microwave spectroscopy revealed fine splittings arising from the internal rotation of the methyl group and hyperfine splittings from the chlorine quadrupole coupling. A global fit using the programs *XIAM* yielded highly accurate molecular parameters with an rms deviation close to measurement accuracy. The A torsional symmetry species lines including the hyperfine components were fitted separately with the program *SPFIT/SPCAT*, showing that treatment of the chlorine quadrupole coupling using first order perturbation theory is at the limit. Comparison with the *RAM36hf* fit proved the sufficiency of *XIAM* in analyzing methyl internal rotation with an intermediate barrier of about 462 cm^{-1} in 2-chloro-4-fluorotoluene. The NQCCs of the chlorine nucleus can be predicted with excellent agreement to experimental values at the B1LYP/TZV(3df,2p)//PBE0/6-31G(3d,3p) level of theory. Comparison of the barrier height and the χ_{cc} NQCC with those of 2- and 3-chlorotoluene has shown that χ_{cc} is somewhat influenced by the methyl position and strongly affected by the presence of the fluorine atom on the phenyl ring, while, very much to the contrary, the latter is of minor importance for the barrier hindering the methyl torsion.

Acknowledgements

The authors thank the Land Niedersachsen and the Deutsche Forschungsgemeinschaft (DFG) for funding. A.L. acknowledges the funding of the Spanish MINECO-FEDER project PGC2018-098561-B-C22. D.A.O. thanks the Alexander von Humboldt Foundation for a post-doctoral fellowship. H.V.L.N. was supported by the Agence Nationale de la Recherche ANR (project ID ANR-18-CE29-0011). Dr. V.V. Ilyushin is greatly acknowledged for his help in performing the *RAM36hf* fits and for making his code available to the spectroscopic community.

References

[1] S. Jacobsen, U. Andresen, H. Mäder, Struct. Chem. 14 (2003) 217.

[2] H.D. Rudolph, A. Trinkaus, Z. Naturforsch. 23a (1968) 68.

[3] J. Rottstegge, H. Hartwig, H. Dreizler, J. Mol. Struct. 478 (1999) 37.

[4] K.P. Rajappan Nair, S. Herbers, H.V.L. Nguyen, J.-U. Grabow, Spectrochim. Acta. A 242 (2020) 118709.

[5] K.P. Rajappan Nair, S. Herbers, J.-U. Grabow, A. Lesarri, J. Mol. Spectrosc. 349 (2018) 37.

[6] K.P. Rajappan Nair, S. Herbers, D.A. Obenchain, J.-U. Grabow, A. Lesarri, J. Mol. Spectrosc. 344 (2018) 21.

[7] K.P. Rajappan Nair, D. Wachsmuth, J.-U. Grabow, A. Lesarri, J. Mol. Spectros. 337 (2017) 46.

[8] K.P. Rajappan Nair, S. Herbers, J.-U. Grabow, J. Mol. Spectrosc. 355 (2019) 19.

[9] K.P. Rajappan Nair, M.K. Jahn, A. Lesarri, V.V. Ilyushin, J.-U. Grabow, Phys. Chem. Chem. Phys. 17 (2015) 26463.

[10] S. Khemissi, H.V.L. Nguyen, ChemPhysChem 21 (2020) 1682.

[11] G. Herberich, Z. Naturforsch. 22a (1967) 761.

[12] V.A. Schubert, D. Schmitz, M. Schnell, Mol.Phys. 111 (2013) 2189.

[13] K.P. Rajappan Nair, K. Epple, Chem.Phys. Lett. 166 (1990)146.

[14] K.P. Rajappan Nair, J.Mol.Struct. 477 (1999) 251.

[15] D. Gerhard, A. Hellweg, I. Merke, W.Stahl, M. Baudelet, D. Petitprez, G. Wlodarczak, J. Mol. Spectrosc. 220 (2003) 234.

[16] K.P. Rajappan Nair, J. Demaison, G. Wlodarczak, I. Merke, J. Mol. Spectrosc. 237 (2006) 137.
[17] S. Herbers, P. Buschmann, J. Wang, K.G. Lengsfeld, K.P. Rajappan Nair, J.-U. Grabow, Phys. Chem. Chem. Phys. 22 (2020) 11490.
[18] K.P. Rajappan Nair, S. Herbers, J.-U. Grabow, A. Lesarri, J. Mol. Spectrosc. 361 (2019) 1.
[19] H. Hartwig, H. Dreizler, Z. Naturforsch. 51a (1996) 923.
[20] R. Kannengießer, M.J. Lach, W. Stahl, H.V.L. Nguyen, ChemPhysChem 16 (2015) 1906.
[21] R.M. Gurusinghe, M.J. Tubergen, J. Phys. Chem. A 120 (2016) 3491.
[22] H.V.L. Nguyen, W. Stahl, J. Chem. Phys. 135 (2011) 024310.
[23] J.M.L.J. Reinartz, W.L. Meerts, A. Dymanus, Chem. Phys. 45 (1980) 387.
[24] A. Belloche, A.A. Mescheheryakov, R.T. Garrod, V.V. Ilyushin, E.A. Alekseev, R.A. Motiyenko, I. Margules, H.S.P. Müller, K.M. Menten, Astron. Astrophys. 601 (2017) A49.
[25] H.M. Pickett, J. Mol. Spectrosc. 148 (1991) 371.
[26] W. Kohn, L. J. Sham, Phys. Rev. A. 140 (1965) 1133.
[27] A.D. Becke, J. Chem. Phys. 98 (1993) 5648.
[28] C.T. Lee, W.T. Yang, R.G. Paar, Phys. Rev. B 37 (1988) 785.
[29] C. Møller, M.S. Plesset. Phys. Rev. 46 (1934) 618.
[30] R. Ditchfield, W.J. Hehre, J.A. Pople, J. Chem. Phys. 54 (1971) 724.
[31] R.J. Bartlett, M. Musial, Rev. Mod. Phys. 79 (2007) 291.
[32] Y. Zhao, D.G. Truhlar, Theor. Chem. Acc. 120 (2008) 215.
[33] J.P. Perdew, M. Ernzerhof, K. Burke, J. Chem. Phys. 105 (1996) 9982.
[34] M.J. Frisch, G.W. Trucks, H.B. Schlegel, G.E. Scuseria, M.A. Robb, J.R. Cheeseman, G. Scalmani, V. Barone, G.A. Petersson, H. Nakatsuji, X. Li, M. Caricato, A.V. Marenich, J. Bloino, B. G. Janesko, R. Gomperts, B. Mennucci, H.P. Hratchian, J.V. Ortiz, A.F. Izmaylov, J.L. Sonnenberg, D. Williams-Young, F. Ding, F. Lipparini, F. Egidi, J. Goings, B. Peng, A. Petrone, T. Henderson, D. Ranasinghe, V.G. Zakrzewski, J. Gao, N. Rega, G. Zheng, W. Liang, M. Hada, M. Ehara, K. Toyota, R. Fukuda, J. Hasegawa, M. Ishida, T. Nakajima, Y. Honda, O. Kitao, H. Nakai, T. Vreven, K. Throssell, J.A. Montgomery, Jr., J. E. Peralta, F. Ogliaro, M.J. Bearpark, J.J. Heyd, E.N. Brothers, K.N. Kudin, V.N. Staroverov, T.A. Keith, R. Kobayashi, J. Normand, K. Raghavachari, A.P. Rendell, J.C. Burant, S.S. Iyengar, J. Tomasi, M. Cossi, J.M.

Millam, M. Klene, C. Adamo, R. Cammi, J.W. Ochterski, R.L. Martin, K. Morokuma, O. Farkas, J.B. Foresman, D.J. Fox, Gaussian 16, Revision B.01, Inc., Wallingford CT, 2016.
[35] W.C. Bailey, J. Mol. Spectrosc. 209 (2001) 57.
[36] W.C. Bailey, Calculation of Nuclear Quadrupole Coupling Constants in Gaseous State Molecules. <http://nqcc.wcbailey.net/index.html>.
[37] R. Kannengießer, W. Stahl, H.V.L. Nguyen, J. Phys. Chem. A 120 (2016) 5979.
[38] J.B. Graneek, W.C. Bailey, M. Schnell, Phys. Chem. Chem. Phys. 20 (2018) 22210.
[39] R. Kannengießer, W. Stahl, H.V.L. Nguyen, W.C. Bailey, J. Mol. Spectrosc. 317 (2015) 50.
[40] R. Hakiri, N. Derbel, W.C. Bailey, H.V.L. Nguyen, H. Mouhib, Mol. Phys. 118 (2020) e1728406.
[41] F.E. Marshall, N. Moon, T.D. Persinger, D.J. Gillcrist, N.E. Shreve, W.C. Bailey, G.S. Grubbs II, Mol. Phys. **117** (2019) 1351.
[42] A.D. Becke, J. Chem. Phys. 104 (1996) 1040.
[43] C. Adamo, V. Barone, Chem. Phys. Lett. 274 (1997) 242.
[44] A. Schäfer, C. Huber, R. Ahlrichs, J. Chem. Phys. 100 (1994) 5829.
[45] D. Feller, J. Comp. Chem. 17 (1996) 1571.
[46] K.L. Schuchardt, B.T. Didier, T. Elsethagen, L. Sun, V. Gurumoorthi, J. Chase, J. Li, T.L. Windus, J. Chem. Inf. Model. 47 (2007) 1045.
[47] P. Pyykkö, J. Li, Nuclear Quadrupole Moments, Report HUKI 1-92, ISSN 0784-0365 (1992).
[48] G.S. Grubbs II, C.T. Dewberry, A. King, W. Lin, W.C. Bailey, S.A. Cooke, J. Mol. Spectrosc. 263 (2010) 127.
[49] J.-U. Grabow, W. Stahl, H. Dreizler, Rev. Sci. Instrum. 67 (1996) 4072.
[50] J.K.G. Watson, in J.R. Durig (Ed.) Vibrational Spectra and Structure, Vol. 6, Elsevier, Amsterdam 1997, pp. 1-89
[51] H.P. Benz, A. Bauder, H.H. Guénthard, J. Mol. Spectrosc. 21 (1966) 156.
[52] S. Grimme, J. Antony, S. Ehrlich, H. Krieg, J. Chem. Phys. 132 (2010) 154104.
[53] T.H. Dunning Jr, J. Chem. Phys. 90 (1986) 1007.